

BeppoSAX Observations of LINER-2 Galaxies

I. Georgantopoulos¹, F. Panessa^{2,3}, A. Akylas^{1,4}, A. Zezas⁵, M. Cappi³, and A. Comastri⁶

¹ Institute of Astronomy & Astrophysics, National Observatory of Athens, Palaia Penteli, 15236, Athens

² Dipartimento di Astronomia, Universita di Bologna, Via Ranzani 1, 40127, Bologna

³ Istituto Tecnologie e Studio delle Radiazioni Extraterrestri/CNR, via Gobetti 101, I-40129, Bologna

⁴ Physics Department, University of Athens, Panepistimiopolis, Zografos, 15783, Athens

⁵ Harvard-Smithsonian Center for Astrophysics, 60 Garden St., Cambridge, MA 02138, U.S.A.

⁶ Osservatorio Astronomico di Bologna, via Ranzani 1, I-40127, Bologna

Received ; accepted

Abstract. We present *BeppoSAX* observations of 6 “type-2” LINER and “transition” galaxies (NGC3379, NGC3627, NGC4125, NGC4374, NGC5195 and NGC5879) from the Ho et al. (1997) spectroscopic sample of nearby galaxies. All objects are detected in the 2-10 keV band, having luminosities in the range $L_{2-10\text{keV}} \sim 1 \times 10^{39} - 1 \times 10^{40}$ erg s⁻¹. The PDS upper limits above 10 keV place constraints on the presence of a heavily obscured AGN in the case of NGC3379 and NGC4125. No significant variability is detected in any of the objects. The spectra are described in most cases by a simple power-law model with a spectral slope of $\Gamma \sim 1.7 - 2.5$ while there is evidence neither for a significant absorption above the Galactic nor for an FeK_{α} emission line. Therefore, based on the spectral properties alone, it is difficult to differentiate between a low-luminosity AGN or a star-forming galaxy scenario. However, imaging observations of NGC3627 and NGC5195 with *Chandra* ACIS-S reveal very weak nuclear sources while most of the X-ray flux originates either in off-nuclear point sources or in diffuse emission. The above clearly argue in favour of a star-forming origin for the bulk of the X-ray emission, at least in the above two sources.

Key words. active – Galaxies: nuclei – Galaxies: starburst X-rays: galaxies

1. Introduction

Low Ionization nuclear emission line regions (LINER) galaxies (Heckman 1980) constitute a significant fraction (33 per cent) of nearby galaxies (Ho, Filippenko & Sargent 1997), and yet the origin of their activity remains under debate. Ho et al. (1997) showed that a small fraction (~ 20 per cent) of LINERs are most probably Active Galactic Nuclei (AGN) as they present broad H_{α} emission line wings in their optical spectra. These were classified as LINER-1, while the remaining LINERs with no broad H_{α} emission were named LINER-2, in analogy with the existing classification of Seyfert galaxies.

The X-ray emission of LINER-2 provides further clues on the origin of these objects. If LINER-2 are also AGN, in analogy with the obscuration model of Seyfert-2 galax-

ies (Antonucci & Miller 1985), their X-ray spectra should show evidence of a strong absorption and large equivalent width FeK emission lines. For example the spectrum of the LINER-1.9 NGC1052 (Weaver et al. 1999) shows obscuration by a large column density ($N_H \sim 3 \times 10^{23}$ cm⁻²) and an FeK line with an equivalent width of 0.3 keV. In contrast, the *BeppoSAX* X-ray spectrum of the LINER-1.9 NGC3998 (Pellegrini et al. 2000) shows neither evidence for obscuration nor for an Fe line. Terashima et al. (2000a) and Roberts, Schurch & Warwick (2001) studied, with *ASCA*, about a dozen of type-2 LINER galaxies from the spectroscopic sample of Ho et al. (1997). The spectra present slopes with typically $\Gamma \sim 1.8$ and no evidence for absorption. Terashima et al. (2000a) and Roberts et al. (2001) find no strong evidence for the presence of an FeK line. Furthermore, Terashima et al. (2000b) find that if LINER-2 are low luminosity AGN (LLAGN), their X-ray luminosities are insufficient to power their H_{α} lumi-

nosities. This suggests an extra source of ionizing radiation (possibly hot stars) or that the AGN, if present, are Compton thick i.e. they are obscured even in the 2-10 keV energy band. In the latter case Terashima et al. (2000b) postulate that we may be observing the scattered component of the nuclear X-ray emission in a similar manner to Compton thick Seyfert-2 galaxies such as NGC1068 (Matt et al 2000). Finally, imaging observations of LINER-2 galaxies using *ROSAT* data (eg Komossa et al. 1999, Roberts et al. 2001) show evidence for extension in soft X-ray energies. Terashima et al. (2000a) report evidence for extension in hard *ASCA* X-ray images of NGC4111 and NGC4569 suggesting that a large fraction of the hard X-ray emission does not originate from an AGN. More recently, Ho et al. (2001) present snapshot observations of a sample of 24 nearby galaxies containing many LINER-2. Their preliminary analysis which is confined to the *nuclear properties*, shows very low levels of nuclear emission in most cases.

Here, we expand significantly the samples of Terashima et al. and Roberts et al. by exploring the X-ray spectral properties of 6 type-2 LINERs from the spectroscopic sample of nearby galaxies of Ho et al. (1997). We perform spectroscopic and variability analysis using the *BeppoSAX* X-ray mission. The majority of the *BeppoSAX* observations are presented here for the first time. Although *ASCA* observations exist for some of our objects, the hard X-ray response of the PDS instrument onboard *BeppoSAX* gives the opportunity to study the X-ray spectra of LINER-2 galaxies in the ultra-hard (>10 keV) X-ray regime. Finally, our *BeppoSAX* analysis is augmented by presenting two public *Chandra* ACIS-S imaging observations of NGC3627 and NGC5195.

2. The sample

We selected LINER-2 objects from the Ho et al. (1997) spectroscopic sample of galaxies which are contained in the public *BeppoSAX* database. The Ho et al. (1997) sample contains medium resolution, high signal to noise nuclear spectra of nearby galaxies ($B_T < 12.5$) in the Northern Hemisphere ($\delta > 0$). We also included transition objects i.e. emission line nuclei whose optical have [OI] strengths intermediate between those of HII nuclei and LINERS (see table 5 of Ho et al. 1997 for the definition of the optical line ratio of the transition objects). Ho et al. (1997) propose that the transition objects can be normal LINERS whose spectra are diluted by nearby HII regions (but see also Barth & Shields 2000). Hereafter, we refer to type-2 LINER and transition objects as LINER-2 galaxies. The sample consists of 6 objects. Although the *BeppoSAX* MECS and LECS data of NGC3379 and NGC4125 have been previously reported by Trinchieri et al. (2000), we re-do the spectral analysis for the sake of uniformity; furthermore the variability as well as PDS spectral analysis are presented here for the first time. Two more low luminosity active galaxies (excluding Seyfert galaxies) from the Ho et al. sample were found in the public *BeppoSAX*

Table 1. The Sample

Name	Classification	Distance Mpc	N_H^{Gal} $\times 10^{20} \text{ cm}^{-2}$
NGC3379	L2/T2	8.1	2.8
NGC3627	T2/S2	6.6	2.4
NGC3998	L1.9	21.6	1.2
NGC4125	T2	24.2	1.8
NGC4374	L2	16.8	2.6
NGC4631	HII	6.9	1.3
NGC5195	L2	9.3	1.6
NGC5879	L2	16.8	1.5

database: NGC3998 and NGC4631; NGC3998 is a LINER-1.9 galaxy whose *BeppoSAX* data have been previously analysed by Pellegrini et al. (2000) while NGC4631 is a star-forming galaxy whose *BeppoSAX* observations, to our knowledge, have not been presented before. We analyse these two galaxies as well in order to compare their properties with those of LINER-2. Table 1 lists our sample: in columns (2), (3) and (4) we give the object classification, distance in Mpc (as given in Ho et al. 1997) and the Galactic column density (Dickey & Lockman 1990) respectively. Throughout this paper we assume a Hubble constant of $H_0 = 75 \text{ km s}^{-1} \text{ Mpc}^{-1}$.

2.1. Summary of recent X-ray observations

2.1.1. NGC3379

This galaxy has been observed by Roberts & Warwick (2000) and Halderson et al. (2001) with good resolution (5 arcsec FWHM) using the HRI onboard *ROSAT* in the soft X-ray energy band (0.1-2 keV). Roberts & Warwick (2000) detect a single source with $L_x \approx 2 \times 10^{39} \text{ erg s}^{-1}$ associated with the galaxy nucleus. NGC3379 has also been observed with *BeppoSAX* by Trinchieri et al. (2000) as part of a sample of early-type galaxies with low L_x/L_B ratios. The *BeppoSAX* spectrum is described by a hard Raymond-Smith (RS) component but with large uncertainties ($kT \sim 7_{-3}^{+17} \text{ keV}$) or with a single power-law with $\Gamma = 1.8_{-0.4}^{+0.3}$.

2.1.2. NGC3627

NGC3627 (M66) is an interacting galaxy in the Leo triplet. It has been previously observed by PSPC onboard *ROSAT* (Dahlem et al. 1996) showing a luminosity of $L_x \sim 5 \times 10^{39} \text{ erg s}^{-1}$ in the 0.1-2 keV band. NGC3627 has also been observed by *ASCA* (Roberts et al. 2001). Its spectrum can be fitted by a two component model: a steep power-law with $\Gamma = 2.6_{-0.37}^{+0.38}$ plus an RS with $kT = 0.88_{-0.07}^{+0.02} \text{ keV}$. NGC3627 has recently been observed by *Chandra* ACIS-S as part of an X-ray imaging survey of nearby galaxies (Ho et al. 2001). The above authors do not detect a nuclear source in NGC3627, giving an upper limit for its luminosity of $L_x < 4 \times 10^{37} \text{ erg s}^{-1}$ in the 2-10 keV

band, an order of magnitude below the *ASCA* luminosity ($L_{2-10\text{keV}} \sim 10^{39} \text{ erg s}^{-1}$) in the same band.

2.1.3. NGC3998

High resolution *ROSAT* HRI observations of NGC3998 (Roberts & Warwick 2000) reveal two bright X-ray sources: one is associated with the nucleus and one off-nuclear source with luminosities (0.1-2 keV) of $L_x \sim 4 \times 10^{41} \text{ erg s}^{-1}$ and $L_x \sim 4 \times 10^{39} \text{ erg s}^{-1}$ respectively. NGC3998 has been observed in hard X-rays by both *ASCA* (Ptak et al. 1999) and *BeppoSAX* (Pellegrini et al. 2000). The *ASCA* spectrum is described well by a single power-law model. The same model described well the *BeppoSAX* data up to 100 keV. No lines were detected, at a statistically significant level, by either *BeppoSAX* or *ASCA*. The *ASCA* X-ray luminosity in the 0.4-10 keV band is $L_x \sim 1 \times 10^{42} \text{ erg s}^{-1}$.

2.1.4. NGC4125

ROSAT PSPC observations of this galaxy (Fabbiano & Schweizer 1995) show some evidence for extended X-ray emission. This galaxy has again been studied by Trinchieri et al. (2000) with *BEppoSAX* in order to determine the origin of the X-ray emission in an early-type galaxy sample. Trinchieri et al. (2000) find a two component fit (RS and blackbody) with temperatures of $kT = 0.3$ and 4 keV respectively.

2.1.5. NGC4374

Halderson et al. (2001) have obtained both *ROSAT* HRI and PSPC observations of this galaxy (M84). The HRI observations reveal a large fraction of extended emission. The X-ray spectrum of this galaxy has been investigated by Matsumoto et al. (1997) using *ASCA*. They find a two component RS fit with temperatures of $kT \sim 10$ and 0.6 keV respectively. Recently, this galaxy has been observed by Ho et al. (2001) and Finoguenov & Jones (2001) using *Chandra*. The galaxy has a nuclear luminosity of $\sim 10^{39} \text{ erg s}^{-1}$ in the 2-10 keV band, more than an order of magnitude lower than the *ASCA* luminosity in the same band. Instead, the majority of the X-ray emission in the hard band, appears to come from off-nuclear point sources and diffuse X-ray emission (Finoguenov & Jones 2001).

2.1.6. NGC4631

ROSAT HRI observations of Roberts & Warwick (2001) resolve the soft X-ray emission into two non-nuclear point sources both with luminosities of $L_{0.1-2\text{keV}} \sim 10^{39} \text{ erg s}^{-1}$. Joint *ASCA* and *ROSAT* PSPC spectral fits (Dahlem, Weaver & Heckman 1998) identify at least three different components: a $\Gamma = 1.9$ power-law, a thermal (MEKAL) component with $kT \sim 0.8$ keV and a softer with $kT \sim 0.2$ keV.

2.1.7. NGC5195

This galaxy interacts with NGC5194 (M51). High resolution observations with *ROSAT* HRI reveal extended X-ray emission and an off-nuclear X-ray source with $L_{0.1-2\text{keV}} \sim 6 \times 10^{38} \text{ erg s}^{-1}$ (Ehle, Pietsch & Beck 1995, Roberts & Warwick 2000, Halderson et al. 2001). NGC5195 is connected to M51 with a bridge of diffuse X-ray emission. The *Chandra* snapshot observations of Ho et al. (2001) do not detect the nucleus giving an upper limit on the 2-10 keV X-ray luminosity of $\sim 10^{38} \text{ erg s}^{-1}$.

2.1.8. NGC5879

This galaxy has not been detected by *EINSTEIN* (Fabbiano, Kim & Trinchieri 1992) yielding an upper limit of $3 \times 10^{40} \text{ erg s}^{-1}$ in the 0.2-4 keV band. No pointed *ROSAT* data exist for this source while the *ASCA* image is contaminated by the nearby radio-loud QSO 1508+5714 (Moran & Helfand 1997).

3. Observations

The scientific instrumentation on board the Italian-Dutch X-ray Satellite *BeppoSAX* includes a Medium Energy Concentrator Spectrometer, MECS, which consists of three units, (Boella et al 1997) a Low Energy Concentrator Spectrometer, LECS, (Parmar et al 1997) a High Pressure Gas Scintillation Proportional Counter, HPGSPC, (Manzo et al 1997) and a Phoswich Detector System, PDS, (Frontera et al 1997), all of which point in the same direction. The MECS instrument consists of a mirror unit plus a gas scintillation proportional counter and has imaging capabilities. It covers the energy range between 2-10 keV with a spatial resolution of about 1.4 arcmin at 6 keV and a spectral resolution of 8 per cent at 6 keV. The three different (or two after May 7 1997, when MECS1 failed) MECS units are merged in order to increase the signal-to-noise ratio. This is feasible because the three MECS units show very similar performance and the difference in the position of the optical axis in the three units is smaller than the scale on which the vignetting of the telescopes varies significantly (>5 arcmin). The LECS instrument is similar to the MECS but operates down to energies of 0.1 keV. The PDS is a direct view detector with rocking collimators and extends the *BeppoSAX* bandpass to high energies (13-300 keV). Its energy resolution is 15 per cent at 60 keV. Finally, HPGSPC detects photons with energies up to 120 keV and has an energy resolution of 4 per cent at 60 keV.

Table 2 lists the exposures times and Sequence Number for all observations. Note that all objects apart from three (NGC4374, NGC5195 and NGC5879), were the observation targets and therefore were observed on-axis. The off-axis angles for each object are listed in the last column of table 2. All objects have been detected in the 2-10 keV band by MECS. We have not used the PDS data in the case of NGC4374, NGC5195 and NGC5879 as there

Table 2. *BeppoSAX* Observation Log

object	date	Sequence No	Exposures (ksec)			Off-axis (arcmin)
			MECS	LECS	PDS	
NGC 3379	1998-12-14	005474	98.4	35.1	50.3	0
NGC 3627	1998-12-19	005488	18.6	18.6	22.4	0
NGC 3998	1999-6-29	006333	76.9	24.9	37.9	0
NGC 4125	1997-4-26	002284	57.2	22.2	22.2	0
NGC 4374	1999-01-22	005519	67.9	66.3	51.2	15
NGC 4631	1997-12-18	003469	97.0	15.0	20.8	0
NGC 5195	2000-1-20	007183	98.9	37.2	44.9	2
NGC 5879	1998-2-1	003751	17.9	7.0	4.2	5

are bright contaminating sources (the observation targets) within the PDS field-of-view. Only NGC3998 is significantly detected with the PDS while no object is detected by the HPGSPC.

4. Short Scale Variability Analysis

The MECS light curves were examined for evidence of short term X-ray variability. We use a binning time of 5 ks. The errors correspond to the 68 per cent confidence level. We have used only objects with adequate photon statistics (> 100 counts). Hence, NGC4374 and NGC5879 were excluded from further variability analysis. We fit the light curve with a constant. The resulting χ^2 imply (see table 3) that there is no statistically significant variability in all cases. As an additional check, we have also performed a Kolmogorov-Smirnov (KS) test. The KS method compares the cumulative distribution of the photon arrival times of the source and the background. Again, no variability has been detected in any of the objects at a confidence level higher than 95 per cent.

Finally, we estimate the variability amplitude by means of the excess variance σ_{rms}^2 (for a definition of this quantity see Nandra et al. 1997). In Fig. 1 we plot the excess variance as a function of the unobscured 2-10 keV luminosity. We compare the variance of the LINER galaxies in our sample to that expected for low luminosity Seyfert galaxies: the solid line represents the extrapolation at low luminosities of the variance-luminosity relation found by Nandra et al. (1997). On Fig. 1 we also present 4 LINER galaxies from the sample of Ptak et al. (1998). It is evident that the LINER galaxies do not show the strong variability amplitude which is expected for Seyfert galaxies in the same luminosity range.

5. Spectral Analysis

We extract the source spectra using a radius of two arcmin. This area encircles more than 85 per cent of the photons at an energy of 3 keV (on-axis). The same extraction radii were used in the LECS case. These correspond to a smaller percentage of enclosed energy in the 0.1-2 keV energy range due to the limited spatial resolution of LECS in the above band. The spectrum of the background was

Table 3. Variability Analysis

Name	count rate $\times 10^{-2}$	χ^2	σ_{rms}^2 $\times 10^{-3}$
NGC 3379	0.3	38/47	-41 \pm 30
NGC 3627	0.8	13/20	-28 \pm 38
NGC 3998	13.4	26/33	-1 \pm 5
NGC 4125	0.2	17/17	-15 \pm 30
NGC 4631	1.0	11/18	-18 \pm 33
NGC 5195	0.4	19/37	-80 \pm 47

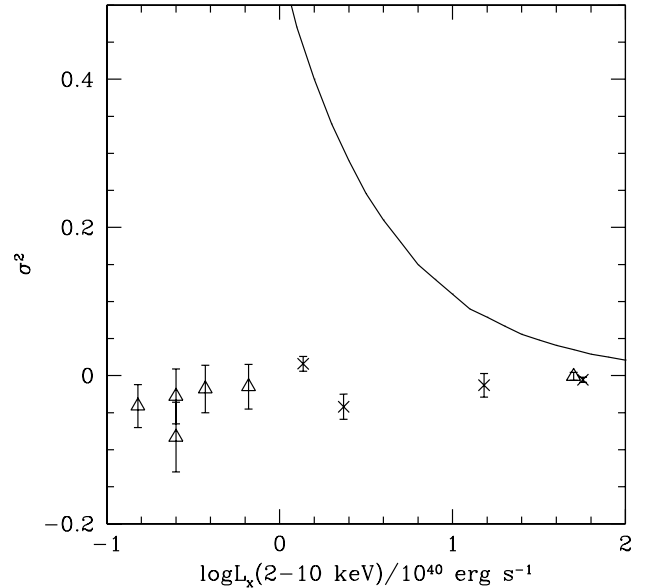


Fig. 1. The excess variance (σ^2) versus luminosity (2-10 keV) for the 6 LINER objects listed in table 3 (open triangles). LINER galaxies from Ptak et al. (1998) are denoted with crosses. The solid line describes the excess variance for Seyfert galaxies derived by Nandra et al. (1997)

estimated from source free regions of the image. We use data between the energy ranges 0.1-4 keV and 2-10 keV for the LECS and MECS detectors respectively where the response matrices are well calibrated. The spectral files

were rebinned linearly to give a minimum of 20 counts per channel. The spectral fitting was carried out using the *XSPEC* v11 software package. The MECS and LECS data were fitted simultaneously. A relative normalization factor was introduced between the LECS and MECS data. We assumed a MECS to LECS normalization factor of 0.90 to account for cross-calibration uncertainties (Fiore, Guainazzi & Grandi 1999).

For each observation, a number of models are applied to the data and for each case the χ^2 statistic is estimated. We first use a single power-law plus neutral absorption model to fit the spectra. Two more complicated models have also been used with the addition of a) a Raymond-Smith (RS), plasma model at soft energies; the temperature was constrained to be $kT < 1$ keV, while the abundance was fixed to 0.1 in agreement with earlier *ASCA* results (Roberts et al. 2001) b) a Gaussian line to account for Fe emission at energies above ~ 6.4 keV; the line width was fixed to $\sigma = 0.001$ keV i.e. unresolved given the MECS spectral resolution.

The best-fit models are presented in Table 4. The best fit spectra together with the residuals for the three objects whose *BeppoSAX* spectra are presented here for the first time (NGC3627, NGC4631, NGC5195) are given in Fig. 2. As explained in more detail in the section below, the single power-law model provides a statistically acceptable fit to most objects. In order to assess the significance of new parameters added to the initial model we have adopted the 99 per cent confidence level using the F-test (Bevington & Robinson 1992). All errors quoted in the best-fit spectral parameters correspond to the 90 per cent confidence level for one interesting parameter.

Finally, we have used the MECS data and the PDS upper limits in order to derive constraints on the presence of a highly absorbed AGN. In particular, we used only the 15–50 keV PDS upper-limits binned into a single bin, to minimize the background. The 15–50 keV 90% upper limits for NGC3379 and NGC4125 are 5×10^{-2} and 6×10^{-2} cts s $^{-1}$ respectively. In the case of NGC3627 where *Chandra* observations show that the level of the nuclear X-ray luminosity is much lower than the total *BeppoSAX* emission, (see next section) the PDS cannot provide powerful constraints. We test how our best-fit models (Table 4) for NGC3379 and NGC4125 are sensitive to the presence of a heavily absorbed (i.e. $N_H > 10^{23}$ cm $^{-2}$) source. We assume that the normalization of such an intrinsic power-law is 20 times higher than the observed power-law normalization. Indeed, this is a typical value for the ratio of scattered to intrinsic X-ray emission in nearby Seyfert-2 galaxies (eg Turner et al. 1997). We further assume the slope of the two power-laws to be identical, but free to vary. Then, by fitting the data, we obtain the following 90 per cent confidence lower-limits on the N_H values: 2 and 1×10^{24} cm $^{-2}$ for NGC3379 and NGC4125 respectively.

5.1. Notes on individual Objects

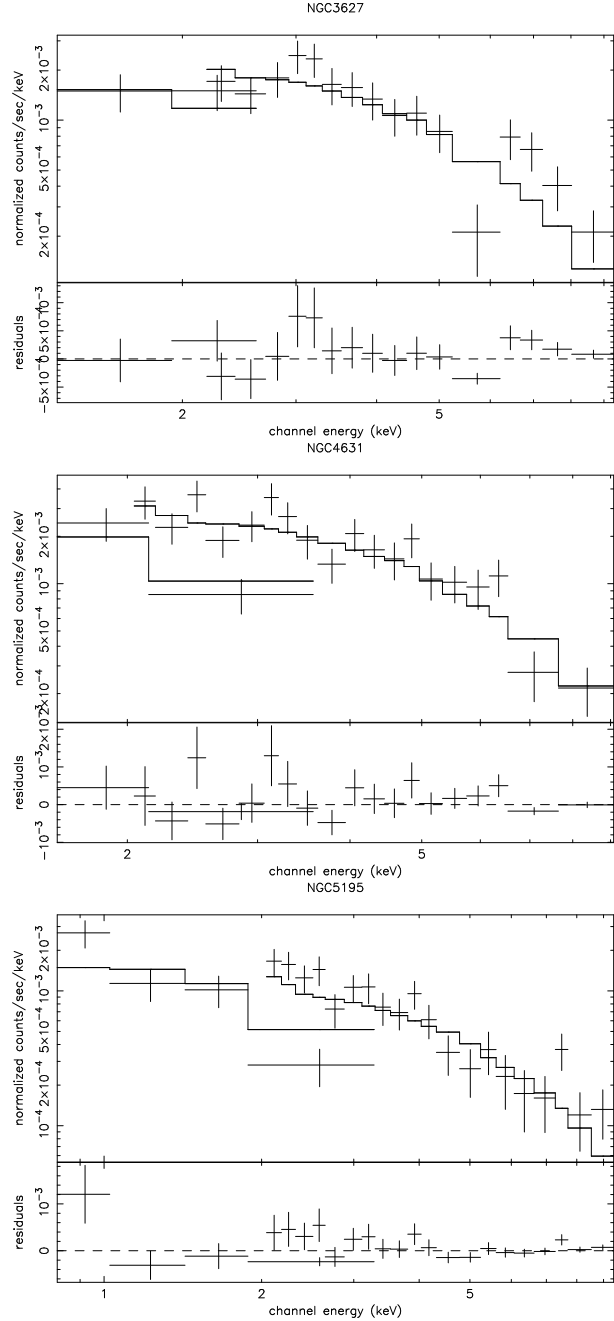


Fig. 2. The spectra (data points, together with the best fit models and residuals) for the three objects (NGC3627, NGC4631 and NGC5195) whose *BeppoSAX* observations are presented here for the first time

5.1.1. NGC3379

The single power-law spectrum provides an acceptable fit with $\chi^2 = 21./16$ degrees of freedom (dof); $\Gamma = 1.65^{+0.44}_{-0.30}$ in agreement with previous results by Trinchieri et al. (2000). The addition of a RS component yields $\Delta\chi^2 \sim 4$ for two additional parameters (normalization and temperature) which does not represent a statistically significant improvement. The addition of a Gaussian line to the single power-law model yields only $\Delta\chi^2 \approx 2.5$ for two additional

parameters. The 90% upper limit for the ew (equivalent width) of the line is ~ 1.5 keV.

5.1.2. NGC3627

The single power-law fit ($\Gamma = 2.35_{-0.60}^{+0.55}$) yields a poor χ^2 (29.8/15 dof) which is rejected at the ~ 98 per cent confidence level. Still, the addition of a RS component (the temperature was set at 0.7 keV) provides no improvement to the fit ($\Delta\chi^2 \sim 0$). The inclusion of an Fe line ($E = 6.78_{-0.16}^{+0.32}$ keV) provides a better fit ($\Delta\chi^2 \sim 7$) but this is significant at only the ~ 90 per cent confidence level for two additional parameters. The 90 % upper limit for the Fe line ew is ~ 2.3 keV. Note that the *ASCAdata* (Roberts et al. 2001) favour instead a two component model (power-law plus RS).

5.1.3. NGC3998

This is the observation with the best signal-to-noise ratio. The PDS data have been included in the spectral fits. More detailed spectral fits on the same *BeppoSAX* data were performed by Pellegrini et al. (2000). A single power-law provides a reasonable fit to the data with $\chi^2 = 300.0/248$. The addition of an RS component ($kT = 0.14_{-0.03}^{+0.04}$ keV) is significant at over the 99 per cent confidence level. The power-law slope is $\Gamma = 1.88 \pm 0.07$ while the column density is $N_H = 0.3_{-0.2}^{+0.1} \times 10^{22} \text{ cm}^{-2}$ i.e. significantly higher than the Galactic column density of $N_H = 0.012 \times 10^{22} \text{ cm}^{-2}$.

5.1.4. NGC4125

The power-law provides an acceptable fit with $\chi^2 = 13.5/10$ dof. The addition of a RS component ($kT = 0.17_{-0.06}^{+0.60}$ keV) yields a better fit with $\Delta\chi^2 \sim 4.5$ for two additional parameters; however this is statistically significant at only the ~ 90 per cent confidence level. Both the power-law slope and the column density are poorly constrained: $\Gamma = 2.52_{-0.55}^{+0.58}$, while the 90 per cent upper limit on N_H is $3 \times 10^{22} \text{ cm}^{-2}$. Unfortunately, no straightforward comparison can be made with Trinchieri et al. (2000) as these authors chose not to fit a power-law model to the data. The addition of an Fe line ($E = 6.75_{-0.35}^{+0.25}$ keV) is significant at just below the 90 per cent confidence level. The ew of the Fe line is largely unconstrained with its 90% upper limit being 7.2 keV.

5.1.5. NGC4374

This source was observed at 15 arcmin off-axis. It is detected at only the 3.2σ level having 71 ± 22 counts. Assuming a power-law spectrum with a $\Gamma = 1.9$ slope, we obtain a 2-10 keV flux of $3.4 \times 10^{-13} \text{ erg cm}^{-2} \text{ s}^{-1}$, corresponding to a luminosity of $\approx 1.1 \times 10^{40} \text{ erg s}^{-1}$.

5.1.6. NGC4631

The spectrum is described by a single power-law model ($\chi^2 = 22.0/18$ dof) with $\Gamma = 2.13_{-0.44}^{+0.52}$ and no significant evidence for an obscuring column density: the 90 per cent uncertainty on N_H is between 0 and $\sim 3 \times 10^{22} \text{ cm}^{-2}$. Both the spectral slope observed as well as the absence of a large obscuring column are typical of the X-ray spectra of both type-1 AGN and nearby star-forming galaxies (eg Ptak et al. 1997, Zezas, Georgantopoulos & Ward 1998). Star-forming galaxies present a RS component at soft energies (with typically $kT \sim 0.7$ keV) due to extended hot gas emission. In the case of NGC4631, the addition of a soft thermal component ($kT \approx 0.22_{-0.10}^{+0.12}$ keV) does not improve the fit ($\Delta\chi^2 \approx 2$), in contrast to the *ROSAT/ASCA* spectral fits of Dahlem et al. (1998). The addition of a Gaussian line to the power-law spectrum is not statistically significant giving $\Delta\chi^2 \sim 3.6$; the 90 % upper limit on the ew is ~ 1 keV.

5.1.7. NGC5195

A single power-law model ($\Gamma = 1.94_{-0.21}^{+0.24}$) provides a reasonable fit to the data ($\chi^2 = 34.6/21$ dof). The addition of a soft RS component with a temperature fixed at 0.7 keV yields only $\Delta\chi^2 = 1.6$ for two additional parameters. The addition of a line instead gives $\Delta\chi^2 = 4.3$. This feature is marginally significant at only the ~ 95 per cent confidence level. The line energy is rather high ($E = 7.61_{-0.28}^{+0.27}$ keV) while its ew is ~ 1.3 keV. Interestingly, Pellegrini et al. (2000) have also detected such a feature in the case of NGC3998 at an energy of $7.4_{-0.2}^{+0.3}$ keV at a low significance level ($< 2\sigma$).

5.1.8. NGC5879

This object is marginally detected at the $\sim 3\sigma$ level. We used a radius of 1 arcmin detection circle to avoid contamination from a nearby (~ 4 arcmin) quasar. This translates to a flux of $8 \times 10^{-14} \text{ erg cm}^{-2} \text{ s}^{-1}$ or to a luminosity of $3 \times 10^{39} \text{ erg s}^{-1}$ in the 2-10 keV band (assuming a spectrum with $\Gamma = 1.9$).

6. Chandra Imaging analysis

6.1. NGC3627

In order to study the spatial properties of the X-ray emission of these galaxies we used archival data obtained with the *Chandra* ACIS-S instrument. Public *Chandra* data exist only for NGC3627 and NGC5195. These have been observed on 3-11-1999 (exposure 1.1 ksec) and on 23-01-2000 (exposure 1.7 ksec) respectively. Preliminary results from these data have been published by Ho et al. (2001), but their study has been focused on the luminosity of the nucleus alone. From the raw data we extracted images in the 0.5-7.0 keV band which were adaptively smoothed. Contours from these images overlaid on DSS optical images of the galaxies are presented in Fig. 3. Source were

Table 4. Best fit spectral models

Name	N_H ($\times 10^{22}$ cm $^{-2}$)	Γ	kT (keV)	χ^2/dof	$L_{2-10\text{keV}}$ ($\times 10^{40}$ erg s $^{-1}$)
NGC3379	$0.05^{+1.05}_{-0.05}$	$1.65^{+0.44}_{-0.30}$	-	21.0/16	0.15
NGC3627	$1.40^{+1.3}_{-1.2}$	$2.35^{+0.55}_{-0.60}$	-	29.8/15	0.25
NGC3998	$0.28^{+0.16}_{-0.11}$	$1.88^{+0.07}_{-0.06}$	$0.14^{+0.04}_{-0.03}$	287.7/248	50.
NGC4125	$0^{+0.32}_{-1.6}$	$2.52^{+0.58}_{-0.55}$	-	13.5/10	0.66
NGC4631	$0.9^{+1.7}_{-0.9}$	$2.13^{+0.52}_{-0.44}$	-	22.0/18	0.37
NGC5195	$0.0^{+0.22}_{-0.21}$	$1.94^{+0.24}_{-0.21}$	-	34.6/21	0.25

Fig. 3. The Chandra ACIS-S contours of NGC5195 (left) and NGC3627 (right) in the 0.5-8 keV band overlaid on Digital Sky Survey images. The diamond and cross represent the position of the UV and radio nucleus respectively. The white vertical bar corresponds to 1 arcmin

detected using the wavelet *WAVDETECT*) algorithm of the *CIAO* v.2.0 software package. In the case of NGC3627, an X-ray point source close to the radio nucleus (offset 2.6 arcsec) is marginally detected. Note that the astrometry error of the *Chandra* images is usually within 2 arcsec and therefore the *Chandra* nuclear X-ray source may be slightly offset from the radio nucleus. More specifically, the coordinates of the nucleus as derived from radio observations (Filho et al. 2001) are $\alpha = 11h20m15.0s, \delta = +12d59m30s$ in J2000 while those of the X-ray source are $\alpha = 11h20m15.1s, \delta = +12d59m28s$ (J2000). The coordinates of the nucleus derived from UV observations, $\alpha = 11h20m15.1s, \delta = +12d59m22s$, J2000, (Maoz et al. 1996) are far off from both the radio and the X-ray source (offset > 6 arcsec). We detect 15 counts from the nucleus translating to an X-ray luminosity of $L_{2-10\text{keV}} \sim 4 \times 10^{37}$ erg s $^{-1}$; we used a radius of 2 arcsec which encompasses over 90 % of the light at 2 keV from an on-axis point source. For the conversion from counts to luminosities we use a power-law model with $\Gamma = 1.9$ absorbed by the Galactic column density. Note that Ho et al. (2001) derive an upper limit of $L_{2-10\text{keV}} \approx 4 \times 10^{37}$ erg s $^{-1}$ for the luminosity of the *radio* nucleus. At least 7 other X-ray point sources are apparently associated with NGC3627. The X-ray emission is dominated by an off-nuclear source (with J2000 coordinates $\alpha = 11h20m20.9s, \delta = +12d58m45s$)

with a luminosity of $L_{2-10\text{keV}} \sim 10^{39}$ erg s $^{-1}$. The 8 point sources (including the nucleus) account for about 60 per cent of the X-ray emission within a radius of 2 arcmin in the 0.5-7 keV band.

6.2. NGC5195

In the case of NGC5195 we observe extended X-ray emission peaking ~ 5 arcsec away from the optical (UV) center of the galaxy. In particular, the X-ray emission peaks at $\alpha = 13h29m59.5s, \delta = +47d15m57s$ while the UV nuclear coordinates are $\alpha = 13h29m59.2s, \delta = +47d15m59s$ (Maoz et al. 1996). The coordinates of the nucleus in the radio are $\alpha = 13h29m59.5s, \delta = +47d15m57s$ according to the NASA Extragalactic Database, (based on VLA observations by Ho & Ulvestad 2001), coincident with the X-ray peak (offset 0.1 arcsec). Given the limited photon statistics it is impossible to discriminate whether this peak corresponds to an additional point source. The nuclear X-ray source has 10 counts (0.5-7 keV) in 2 arcsec region (assuming it is pointlike), translating to a luminosity of $L_{2-10\text{keV}} \sim 2 \times 10^{38}$ erg s $^{-1}$. Thus it contributes only a small fraction of the total galaxy X-ray emission. The brightest source has a luminosity of $L_{2-10\text{keV}} \sim 3 \times 10^{38}$ erg s $^{-1}$ while strong diffuse X-ray emission can be clearly seen up to 40 arcsec (1 kpc) with $L_{2-10\text{keV}} \sim 10^{39}$ erg s $^{-1}$.

Note that the derived nuclear luminosity in the case of NGC5195 lies above the upper limit of Ho et al. (2001). This discrepancy is probably explained by the different nuclear positions used by us and Ho et al. (2001). Indeed, in the case of NGC5195, Ho et al. (2001) use the optical nuclear coordinates from the POSS plate while we are using the coordinates of the central X-ray source (which we assume to be coincident with the radio nucleus within the errors of the Chandra astrometry).

7. Discussion & Conclusions

The spectra of all our LINER-2 objects are well described by a single power-law with $\Gamma \sim 1.7 - 2.5$. This spectral slope is typical of both LLAGN (Ptak et al. 1999) as well as star-forming galaxies (eg Dahlem et al. 1998). Interestingly, our two comparison objects, NGC3998 and NGC4631, a bona-fide AGN and star-forming galaxy respectively according to their high quality optical spectra, again present similar X-ray spectra. It is evident that it is quite difficult to differentiate between the low-luminosity AGN and the star-forming scenario on the basis of the X-ray continuum alone. The FeK emission line could offer instead a powerful diagnostic. For example the presence of an FeK line at 6.4 keV is frequently used as a definitive proof for the presence of an AGN. Moreover, narrow ionized Fe emission lines due to hot gas around 6.7 keV are more characteristic of star-forming galaxies (eg M82, Ptak et al. 1997; NGC253, Persic et al. 1998). Unfortunately, the limited photon statistics did not allow the detection of any of the above spectral features in our objects. If the X-ray emission in LINER-2 galaxies emanates mainly from star-forming processes we would expect a strong soft component with a temperature of ~ 0.7 keV. Such a component arises from supernova driven superwinds and appears to be ubiquitous in star-forming galaxies independent of their luminosity (Ptak et al. 1997, Zezas et al. 1998). We found no strong evidence for the presence of a soft component in our objects (apart for the LINER 1.9 galaxy NGC3998 where the temperature of the RS component is much softer with $kT \sim 0.2$ keV). We believe that a soft component due to hot gas may be actually present but unfortunately the limited signal-to-noise of the LECS observations coupled with uncertainties in the relative cross-calibration of MECS and LECS hamper its detection. Indeed, *ASCA* observations of NGC3627 (Roberts et al. 2001) and NGC4631 (Dahlem et al. 1998) detect soft X-ray emission with $kT \sim 0.7$ keV in both objects.

Comparison of the X-ray luminosity and the optical H_α luminosity yields more clues on the ionizing source in these objects. Indeed, Terashima et al. (2000b) using *ASCA* observations of several LINER-2 galaxies found that their X-ray emission is insufficient to produce the observed H_α luminosities. According to Terashima et al. (2000b) this means that either an additional ionizing radiation is present (eg hot stars) or that the nucleus is heavily obscured below 10 keV. In Fig. 4 we compare the X-ray

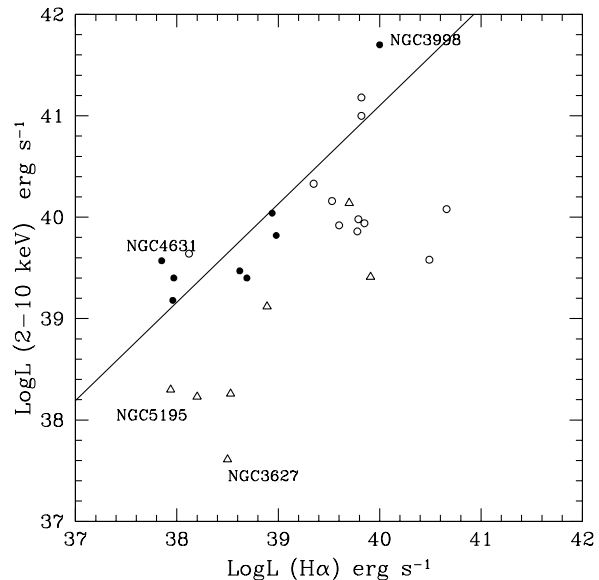


Fig. 4. The X-ray luminosity (2-10 keV) versus the narrow H_α luminosity for the LINER-2 objects in our sample (filled circles), in Terashima et al. (2000b) (open circles). The *Chandra* nuclear luminosities of NGC3627 and NGC5195 as well as several other galaxies from the sample of Ho et al. (2001) are also shown (open triangles). The solid line denotes the $L_x - L_{H_\alpha}$ relation holding for type-1 AGN from Terashima et al. (2000b).

luminosities against the H_α luminosities for our sample. The H_α luminosities were taken from Ho et al. (1997). We use the narrow component luminosity correcting for the effects of reddening (see Ho et al. 1997 for details). The objects from Terashima et al. (2000b) are also given on this plot. The solid line gives the best fit line for type-1 AGN (QSOs, Seyfert-1 and LINER-1) from Terashima et al. (2000b). We have also plotted the *Chandra* nuclear X-ray luminosities for LINER-2 galaxies from Ho et al. (2001), (detections only), as well as our *Chandra* nuclear luminosities for NGC3627 and NGC5195. Most of our *BeppoSAX* luminosities follow the type-1 AGN line. However, this result appears to be rather coincidental as all the *Chandra* nuclear X-ray luminosities lie below the type-1 AGN correlation confirming the claims of Terashima et al. (2000b). It is evident that the large aperture of *ASCA* and *BeppoSAX* (a few arcminutes) compared to that used for the optical spectroscopy (2×4 arcsec) alter the true form of the $L_x - L_{H_\alpha}$ relation. The high energy response of the MECS and PDS instruments gives the opportunity to check whether the low X-ray luminosities could be due to high amounts of obscuration. In the case of NGC3379, NGC3627 and NGC4125, we find that the MECS and PDS data are inconsistent with a column density as high as $\sim 10^{24} \text{ cm}^{-2}$. If these sources have to be heavily obscured then the obscuring material should have an even larger column and the three sources should have to be Compton thick. Alternatively, a more plausible

scenario is that hot stars are providing the UV continuum necessary to produce the observed H_{α} luminosities. Maoz et al. (1995) and Barth et al. (1998) find that about 25 per cent of LINER galaxies display a compact nuclear UV source. In a fraction of these, the *HST* UV spectra clearly show absorption line signatures of massive stars indicating a stellar origin for the UV continuum (Maoz et al. 1998).

Perhaps, more conclusive evidence on the origin of the X-ray emission in these objects comes from the *Chandra* imaging analysis. The images of NGC3627 and NGC5195 presented here, show a very weak nuclear emission with most of the flux arising instead in either off-nuclear sources or in diffuse emission. Similar conclusions are reached on the basis of the *Chandra* image of NGC4374 (Finoguenov & Jones, 2001). These properties are reminiscent of nearby star-forming galaxies such as M82 and NGC253 (Kaaret et al. 2001, Pietsch et al. 2001, Strickland et al. 2000) where the bulk of the X-ray emission originates in off-nuclear sources. Of course it remains to be seen whether the other objects in our sample present similar imaging properties to NGC3627 and NGC5195.

In conclusion, the spectral *BeppoSAX* observations are consistent with both an unobscured LLAGN and a star-forming galaxy scenario. The key test is provided by the *Chandra* imaging observations which clearly reveal that the a large fraction of the X-ray emission is provided by star-forming processes at least in the case of NGC3627 and NGC5195, where the bulk of the X-ray luminosity has an off-nuclear origin. These observations cannot rule out the presence of a LLAGN in these galaxies. However, in this case the nuclear luminosity should be comparable to that of an X-ray binary, unless the nucleus is heavily obscured. Future, longer exposure *Chandra* and *XMM* observations will be able to perform spatially resolved spectroscopy of the nuclear regions. The detection of emission lines is expected to provide powerful diagnostics on the nature of the nuclear emission.

Acknowledgements. We are grateful to the referee Dr. Y. Terashima for his numerous comments and suggestions. The project was funded by a Greek-Italian scientific bilateral agreement under the title “Observations of active galaxies with the Italian astrophysics mission *BeppoSAX*”, funded jointly by the Greek General Secretariat for Research and Technology and the Italian Foreign Ministry. AZ acknowledges support from grant NAS 8-39073. This work has made use of data obtained from the *BeppoSAX* Science Data Center.

References

- Antonucci, R.R.J., Miller, J.S., 1985, 297, 621
 Barth, A., Ho., L.C., Filippenko, A.V., Sargent, W.L.W., 1998, *ApJ*, 496, 133
 Barth, A.J., Shields, J.C., 2000, *PASP*, 112, 753
 Bevington, P.R., Robinson, D.K., 1992, *Data Reduction and Error Analysis for the Physical Sciences*, McGraw-Hill, New York
 Boella G. et al, 1997, *A&AS*, 122, 327
 Dahlem, M., Heckman, T.M., Fabbiano, G., Lehnert, M.D., Gilmore, D., 1996, *ApJ*, 461, 724
 Dahlem, M., Weaver, K., Heckman, T.M., 1998, *ApJS*, 18, 401
 Dickey, J.M., Lockman, F.J., 1990, *ARA&A*, 28, 215
 Ehle, M., Pietsch, W., Beck, R., 1995, *A&A*, 295, 289
 Fabbiano, G., Kim, D.-W., Trinchieri, G., 1992, *ApJS*, 80, 531
 Fabbiano, G., Schweizer, F., 1995, *ApJ*, 447, 572
 Filho, M.E., Barthel, P.D., Ho, L.C., 2000, *ApJS*, 129, 93
 Finoguenov, A., Jones, C., 2001, *ApJ*, 547, L107
 Fiore, F., Guainazzi, M., Grandi, P., 1999, *Handbook for BeppoSAX NFI spectral analysis*, ftp://www.sdc.asi.it/pub/sax/docs/saxabc_v1.2.ps.gz
 Frontera F., Gosta E., dal Fiume D., Feroci M., Nicastro L., Orlandini M., Palazzi E., Zavattini G., 1997, *A&AS*, 122, 357
 Halderson, E.L., Moran, E.C., Filippenko, A.V., Ho, L.C., 2001, *AJ*, 122, 637
 Heckman, T.M., 1980, *A&A*, 87, 142
 Ho, L.C., Filippenko, A.V., Sargent, W.L.W., 1997, *ApJ*, 112, 315
 Ho, L.C. et al., 2001, *ApJ*, 549, L51
 Ho, L.C. & Ulvestad, J.S., 2001, *ApJS*, 133, 77
 Kaaret, P., Prestwich, A.H., Zezas, A., Murray, S.S., Kim, D.W., Kilgard, R.E., Schlegel, E.M., Ward, M.J., 2001, *MNRAS*, 321, L29
 Komossa, S., Bohringer, H., Huchra, J.P., 1999, *A&A*, 349, 88
 Manzo G., Giarrusso S., Santangelo A., Ciralli F., Fazio G., Piraino S., Segreto A., 1997 *A&AS*, 122, 341
 Maoz, D., Filippenko, A.V., Ho, L.C., Rix, H.W., Bahcall, J., Schneider, D.P., Macchetto, F.D., 1995, *ApJ*, 440, 91
 Maoz, D., Filippenko, A.V., Ho, L.C., Macchetto, F.D., Rix, H., Schneider, D.P., 1996, *ApJS*, 107, 215
 Maoz, D., Koratkar, A., Shields, J.C., Ho, L.C., Filippenko, A.V., Sternberg, A., 1998, *AJ*, 116, 55
 Matsumoto, H., Koyama, K., Awaki, H., Tsuru, T., Loewenstein, M., Matsushita, K., 1997, *ApJ*, 482, 133
 Matt, G., Fabian, A.C., Guainazzi, M., Iwasawa, K., Bassani, L., Malaguti, G., 2000, *MNRAS*, 318, 173
 Moran, E.C., Helfand, D., 1997, *ApJ*, 484, L95
 Nandra, K., George, I.M., Mushotzky, R.F., Turner, T.J., Yaqoob, T., 1997, *ApJ*, 476, 70
 Parmar A.N., Martin D.D.E., Bavdaz M., Favata F., Kuulkers E., Vacanti G., Lammers U., Peacock A., Taylor B.G., 1997 *A&AS*, 122, 309
 Persic, M., et al. 1998, *A&A*, 339, L33
 Pellegrini, S., Cappi, M., Bassani, L., della Ceca, R., Palumbo, R., 2000, *A&A*, 360, 878
 Pietsch, W., et al., 2001, *A&A*, 365, L174
 Ptak, A., Serlemitsos, P., Yaqoob, T., Mushotzky, R., Tsuru, T., 1997, *AJ*, 113, 1286
 Ptak, A., Yaqoob, T., Mushotzky, R., Serlemitsos, P., Griffiths, R., 1998, *ApJ*, 501, L37
 Ptak, A., Serlemitsos, P., Yaqoob, T., Mushotzky, R., 1999, *ApJS*, 120, 179
 Roberts, T.P., Warwick, R.S., 2000, *MNRAS*, 315, 98
 Roberts, T.P., Surch, N.J., Warwick, R.S., 2001, *MNRAS*, 324, 737
 Strickland, D.K., Heckman, T.M., Weaver, K.A., Dahlem, M., 2000, *AJ*, 120, 2965
 Terashima, Y., Ho, L.C., Ptak, A.F., Mushotzky, R.F., Serlemitsos, P.J., Yaqoob, T., Kunieda, H., 2000a, *ApJ*, 533, 729
 Terashima, Y., Ho, L.C., Ptak, A.F., 2000b, *ApJ*, 539, 161
 Trinchieri, G., Pellegrini, S., Wolter, A., Fabbiano, G., Fiore, F., 2000, *A&A*, 364, 43

- Turner, T.J., George, I.M., Nandra, K., Mushotzky, R.F., 1997,
ApJ, 488, 164
- Weaver, K.A., Wilson, A.S., Henkel, C., Braatz, J.A., 1999,
ApJ, 520, 130
- Zezas, A., Georgantopoulos, I., Ward, M.J., 1998, MNRAS,
301, 915

This figure "fig3_ngc3627.gif" is available in "gif" format from:

<http://arxiv.org/ps/astro-ph/0202189v1>

This figure "fig3_ngc5195.gif" is available in "gif" format from:

<http://arxiv.org/ps/astro-ph/0202189v1>